

RECEIVED BY
FRACTURE RESISTANCE OF RANDOM FIBER GLASS
COMPOSITES (Indian Inst. of Tech.) 29 p HC
DRAFT A03/MF 801

379-22212

Enclosed
8/2/24 34963

FRACTURE RESISTANCE OF RANDOM FIBER GLASS COMPOSITES
 ESA-SDS Aero

A. C. GARG and C. K. TROTMAN**

ABSTRACT

The concept of crack growth resistance curve (R-curve) has been applied to random fiber glass composites and analytical relations for R-curves have been obtained. The effect of thickness and the procedure of lamination is studied. It is found that thickness does not affect significantly the fracture characteristics. The analytical relations for R-curve are used to predict the residual strength characteristics and the fracture toughness.

INTRODUCTION

Gagger and Broutman⁽¹⁾ have applied the crack growth resistance method for random fiber polystyrene composites and showed that the K_R -curve is independent of initial crack length. Based upon their study they concluded that the K_R -curve concept could be an useful approach to study the fracture behaviour of such materials since substantial amount of slow crack growth occurs prior to unstable fracture.

19960220
130

REF ID: A63198

* Aero. Engg. Dept., I.I.T. Powai, Bombay -400 076, India.

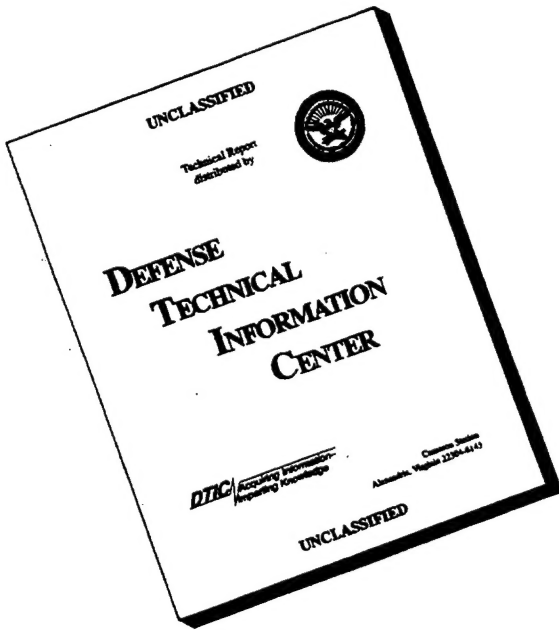
** College of Aeronautics, Cranfield Institute of Technology, Cranfield, England.

DEPARTMENT OF DEFENSE
PLASTICS TECHNICAL EVALUATION CENTER
ARRADCOM, DOVER, N. J. 07801

DISTRIBUTION STATEMENT A

Approved for public release;
Distribution Unlimited

DISCLAIMER NOTICE



**THIS DOCUMENT IS BEST
QUALITY AVAILABLE. THE
COPY FURNISHED TO DTIC
CONTAINED A SIGNIFICANT
NUMBER OF PAGES WHICH DO
NOT REPRODUCE LEGIBLY.**

More recently Morris and Hahn⁽²⁾ have applied the K_R -curve approach to graphite/epoxy composites where they have shown that the effective increment of crack length at fracture and the corresponding K_R are independent of initial crack length.

This paper too attempts to characterise the fracture behaviour of fiber reinforced glass composites using R-curve approach and obtains the analytical relations for R-curves. An approximate relation for critical stress intensity factor (fracture toughness K_c) is presented.

MATERIAL PREPARATION AND EXPERIMENTAL PROCEDURE :

The specimens used in the experimental program were prepared by Preodorite Ltd., U.K. using Chopped Strand Mat (CSM) in Z-7 Rigid resin. The laminations designated as A, B and C were prepared in the following manner :

A : 4 layers of $.45 \text{ kg/m}^2$ CSM in Z-7 Rigid resin (thickness $\approx 3.5 \text{ mm}$).

B : 16 layers of $.45 \text{ kg/m}^2$ CSM in Z-7 Rigid resin (thickness $\approx 13 \text{ mm}$).

C : 16 layers of $.45 \text{ kg/m}^2$ CSM in Z-7 Rigid resin, prepared over a period of 4 days curing 4 layers of CSM in resin each day. (thickness $\approx 13 \text{ mm}$).

The specimens were cut to size of about 125 x 600 mm and provided with an edge notch by means of .5 mm saw. This was further sharpened using a .15 mm saw. All specimens were tested under load-controlled conditions in an Avery Denison fatigue testing machine. During each test the applied load and pseudocrack opening displacement (COD) were monitored and recorded continuously on an X-Y plotter. The COD was measured by a double cantilever clip gage⁽³⁾ as shown in Fig.1.

The load-COD curves as recorded are given in Figures 2,3, and 4 for laminates A, B and C respectively. These curves are found to be linear initially followed by almost continuous deviation from linearity indicating a slow crack growth prior to fracture. Since the composites tested do not show any visible self similar crack growth such as occurs in metals, an effective crack length matching the compliance based on COD was used to construct crack growth resistance R-curves. The compliance was obtained using the initial straight portion of load displacement records at various initial crack lengths. This compliance was plotted against a/w as shown in Fig.5 to obtain the effective crack lengths. The procedure to obtain effective crack length is as follows:

- 1) As shown in Fig.6, a straight line is drawn from the origin to the selected point on the load-displacement curve. The Inverse of the slope of this line is the compliance.

2) Using this compliance together with the calibration curve (Fig.5) gives the effective crack length. The procedure can be repeated for other points on the load-COD curve to get additional values of effective crack lengths.

EVALUATION OF R-CURVES:

Crack growth resistance - R is defined as

$$R = \frac{K_R^2}{E} = \frac{1}{E} Y^2 \sigma^2 a, \quad \dots (1)$$

where,

a is the effective instantaneous crack length corresponding to stress σ ,

Y is finite width correction factor defined by

$$Y = 1.99 - .41(a/w) + 18.7(a/w)^2 - 38.48(a/w)^3 + 53.85(a/w)^4 \quad \dots (2)$$

and E is the Young's modulus of the material.

The variations of K_R^2 with effective crack length a are shown in figure 7 to 9 for laminates A, B and C respectively. The figures indicate that the K_R - effective crack length relationships appear to be nonlinear. From Fig.9 it is seen that the K_R - curves are similar for all the initial crack lengths. The maximum value of K_R do not vary significantly with initial crack length but K_R at crack growth initiation varies to some extent. This

indicates that crack growth resistance may be independent of initial crack length which is confirmed by Fig.12 where K_R^2 has been plotted as a function of crack extension ($\Delta a = a - a_0$) for laminates B. The scatter from mean line is small.

From Figures 7 and 9 it is difficult to make such conclusive statement as to whether one could consider K_R to be independent of initial crack length as all the panels do not lead to consistent K_R behaviour, though maximum K_R does not vary significantly except in a few cases.

Superposition of Figures 7 and 8 reveals that the K_R curve for atleast $a_0/w = 0.2$ is almost identical, indicating that crack growth resistance may be independent of laminate thickness. However, more data will be needed to substantiate this statement. Despite such variations, the interesting feature of these results is that the average of maximum K_R (denoted as K_{R_f} in Table III) is practically same for laminates A, B and C respectively.

The R-curves can be used to predict the crack instability point by plotting the crack driving force curves with σ as a parameter (Fig.10) using the equation

$$K^2 = Y^2 \sigma^2 a \quad \dots (3)$$

In Figures 7, 8 and 9 where such curves have not been actually shown. The point of tangency between R-curves and crack driving force curve determines the point of instability. For the present cases such points of tangency were not observed in all cases. Thus in such cases the maximum value of K_R (denoted as K_{R_f}) is considered as critical which are represented by K_{R_t} in Table III. The average K_{R_t} are found to be practically same for laminates A, B and C indicating that K_R value at instability is invariant with thickness and the procedure of lamination.

These R-Curves can also be used to calculate candidate stress intensity factor K_Q using a crack extension of 2δ of intial crack length similar to one used by Jones and Brown⁽⁴⁾ for some metallic materials. The values of K_Q so determined are indicated in Table III and are found to be varying with initial crack length. Due to such variation probably K_Q may not be treated as a characteristic parameter as critical stress intensity factor. Also indicated in this table are the values of K_{max} obtained on the basis of maximum load and initial crack length. The average K_{max} do not differ very much between laminates A, B and C.

Kraft et.al⁽⁵⁾ have proposed R-curves to be invariant i.e. independent of intial crack length. Then R-curve would be a function only of the amount of

slow crack growth Δa . To verify this statement the variation of K_R^2 with effective crack extension $\Delta a/w$ are plotted on double logarithm scale in Figs. 11, 12 and 13. It is depicted from these figures that there is linear relationship between $\log K_R^2$ and $\log (\Delta a/w)$. Using the method of least squares the mean lines were determined and are shown on these figures. It is obvious that the deviation from the mean lines is small and is almost negligible in the case of laminates B. In view of small deviation, R-curve can be considered to be function of Δa only and may be represented by simple power law

$$R = \frac{K_R^2}{E} = \frac{1}{E} \beta (\Delta a/w)^\alpha \quad \dots (4)$$

where α and β for laminates A, B and C are given by Table I.

TABLE -1
Constants for R-curve equation

Laminates	α	β (MN/m)
A	.40	539.5
B	.29	396.1
C	.46	501.2

R-curves so determined, are shown in Fig.14 as K_R^2 vs. a/w . It is observed that R-curves for laminates A and B do not differ significantly from each other but differ considerably from laminates C. As a result, R-curve may be considered invariant with thickness but not with procedure of laminations. In view of small variation between A and B an equation

$$K_R^2 = 467.7 (\alpha a/w)^{3.45} \quad \dots (5)$$

can be used to represent R-curve for laminates of any thickness without causing appreciable error. This curve is shown in Fig.14 as an average of A and B. The analytical expression(4) for R can be used to derive fracture criterion by using the fracture conditions

$$\begin{aligned} G &= R \\ \frac{\partial G}{\partial a} &= \frac{\partial R}{\partial a} \end{aligned} \quad \dots (6)$$

where G is the energy release rate and is given by,

$$G = \frac{K^2}{E} = \frac{\sigma^2 Y^2 a}{E} \quad \dots (7)$$

These equations lead to the following fracture criterion

$$a_0 = a_c (1-\alpha) F_2/F_1 \quad \dots (8)$$

$$\sqrt{a_c} = \sqrt{\beta} (\alpha a_c / F_1 \omega)^{\alpha/2} Y^{-1} \quad \dots (9)$$

where.

$$F_1 = 1 + 2 a_c Y (wY)^{-1} \quad \dots (10)$$

$$F_2 = 1 + 2 Y a_c Y(1-\alpha) w^{-1} \quad \dots (11)$$

$$Y'' = \gamma Y / \gamma(a/w) \mid a = a_c \quad \dots (12)$$

a_0 and a_c are initial and critical crack length respectively and Y is given by equation (2).

The equations (8) and (9) lead to the determination of critical stress σ_c and critical crack length a_c .

When edge effects are negligible i.e. $Y'' = 0$ and $Y = \text{const}$, the equations (8) and (9) yield

$$a_c = a_0 / (1-\alpha) \quad \dots (13)$$

$$\text{and} \quad \sigma_c a_c^{(1-\alpha)/2} = \text{const} \quad \dots (14)$$

which are identical to one derived by Brock^(6,p.188).

To show the usefulness of equations (8) and (9) a_c/w and σ_c have been plotted as functions a_0/w in Figs. 15 and 16 where they are compared with test results. The agreement between calculated and test results is good. Figure 16 also indicates that σ_c varies little with thickness. These figures may be useful in predicting the residual strength of such laminates.

The equations (5) and (6) can be used to determine critical stress intensity factor K_c corresponding to critical strain energy release rate G_c as a function of a_c . Such behaviour of K_c is shown in Figure-17 which indicates that the variation of K_c with a_c/w is small.

Figure 15 depict the linear behaviour of a_c/w with a_c/w for $a_c/w > .15$ so that

$$a_c/w \approx m(a_c/w) + c_1, \quad a_c/w > .15$$

... (15)

where m and c_1 are given by Table -II.

TABLE -II

Constants for eqn. for critical crack length a_c

Laminates	m	c_1
A	.955	.0625
B	.970	.045
C	.965	.0675

Since variation of a_c/w with thickness in Figure 15, appears to be small, a single line

$$a_c/w = .9625(a_c/w) + .05375, \quad a_c/w > .15 \quad \dots (16)$$

may be used to represent laminates A and B within small

error. Thus we may get an approximate relationship for critical stress intensity factor K_c using equations (16) and (5) as

$$K_c = 13.06 \cdot 1725 \{1 - 7 a_0/w\} , a_0/w > 15 \quad \dots (17)$$

which may be considered as a fracture toughness parameter.

CONCLUSIONS :

1. Due to slow crack growth prior to fracture, R-curves are found to be useful to provide full information on the fracture resistance of the material upto the final fracture.
2. Average value of K_R at point of instability is practically same for all laminates.
3. The effective crack growth at instability point varies with initial crack length and the extension in general is large in case of laminates C. This indicates that the critical stress for laminates C should be smaller than laminates A or B. Thus it appears disadvantageous to prepare laminations with large interval of times.
4. A simplified expression for critical stress intensity factor or fracture toughness K_c is given by eqn.(17) which may be found useful for quick estimation of fracture toughness for such materials.

ACKNOWLEDGEMENTS :

The first author would like to acknowledge the support of the Association of Commonwealth Universities, U.K., through the commonwealth scholarship program to carry out the work at Cranfield Institute of Technology, England. The authors would also like to thank Prodorite Ltd., U.K. for providing the material for testing and Cranfield Institute of Technology for experimental facilities.

REFERENCES :

1. S.K.Gagger and L.J.Breutman, "Strength and Fracture Properties of Random Fiber Polyester Composites", *Fiber Science and Technology*, 9, 205-224 (1976).
2. D.H.Morris and H.T. Hahn, "Fracture Resistance Characterisation of Graphite/Epoxy Composites", *Composite Materials Testing and Design*", ASTM STP 617, 5-17 (1977).
3. W.F.Brown and J.E. Srawley, "Plane Strain crack toughness testing of high strength metallic materials", *ASTM STP 410*, 1966.
4. M.H.Jones and W.F.Brown, "The influence of crack length and thickness in plane strain fracture toughness tests", *ASTM STP 463*, ASTM, Philadelphia, 1970.
5. J.M.Kraft, A.M.Sullivan and R.W.Boyle, "Effect of dimensions on fast fracture instability of notched sheets" *Proc. of the crack propagation symposium*, 1, pp.8-26, Cranfield, 1961.
6. D.Brock, "Elementary Engineering Fracture Mechanics" Noordhoff International Publishing Leyden, Netherlands, 1974.

0000

→ 120 Ω wire resistance
strain gage

600



→ Digital voltmeter
and X-Y recorder

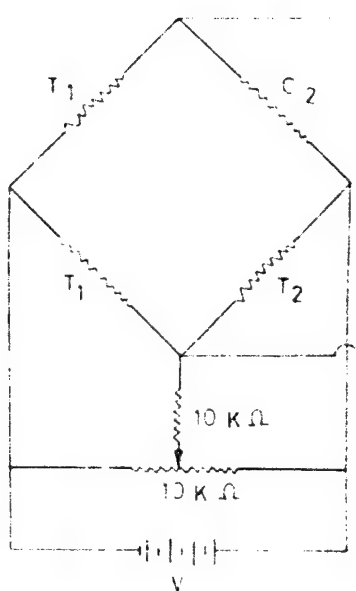


Fig.1 Specimen and the clip gage.

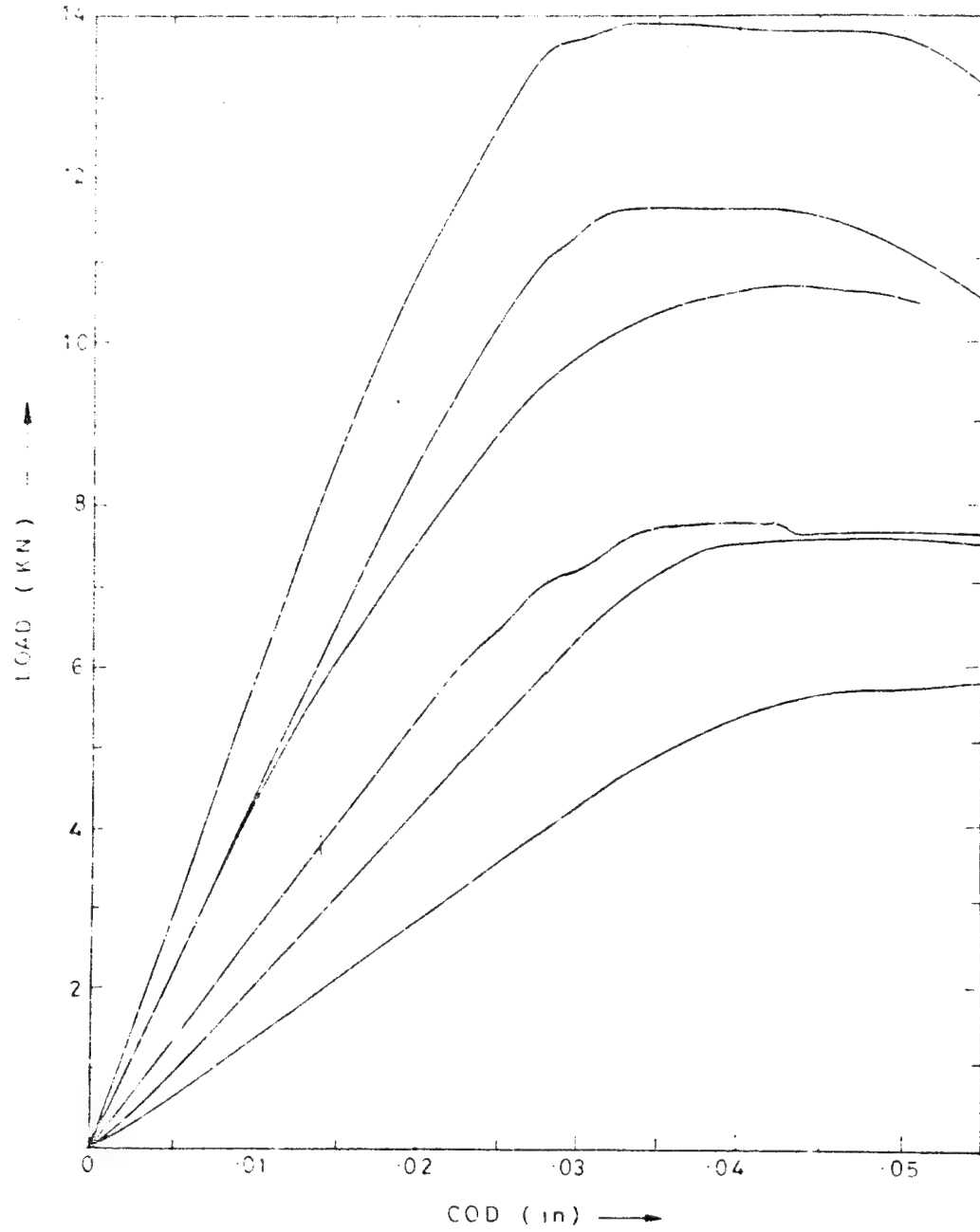


Fig. 2 .Load displacement record for laminate A .

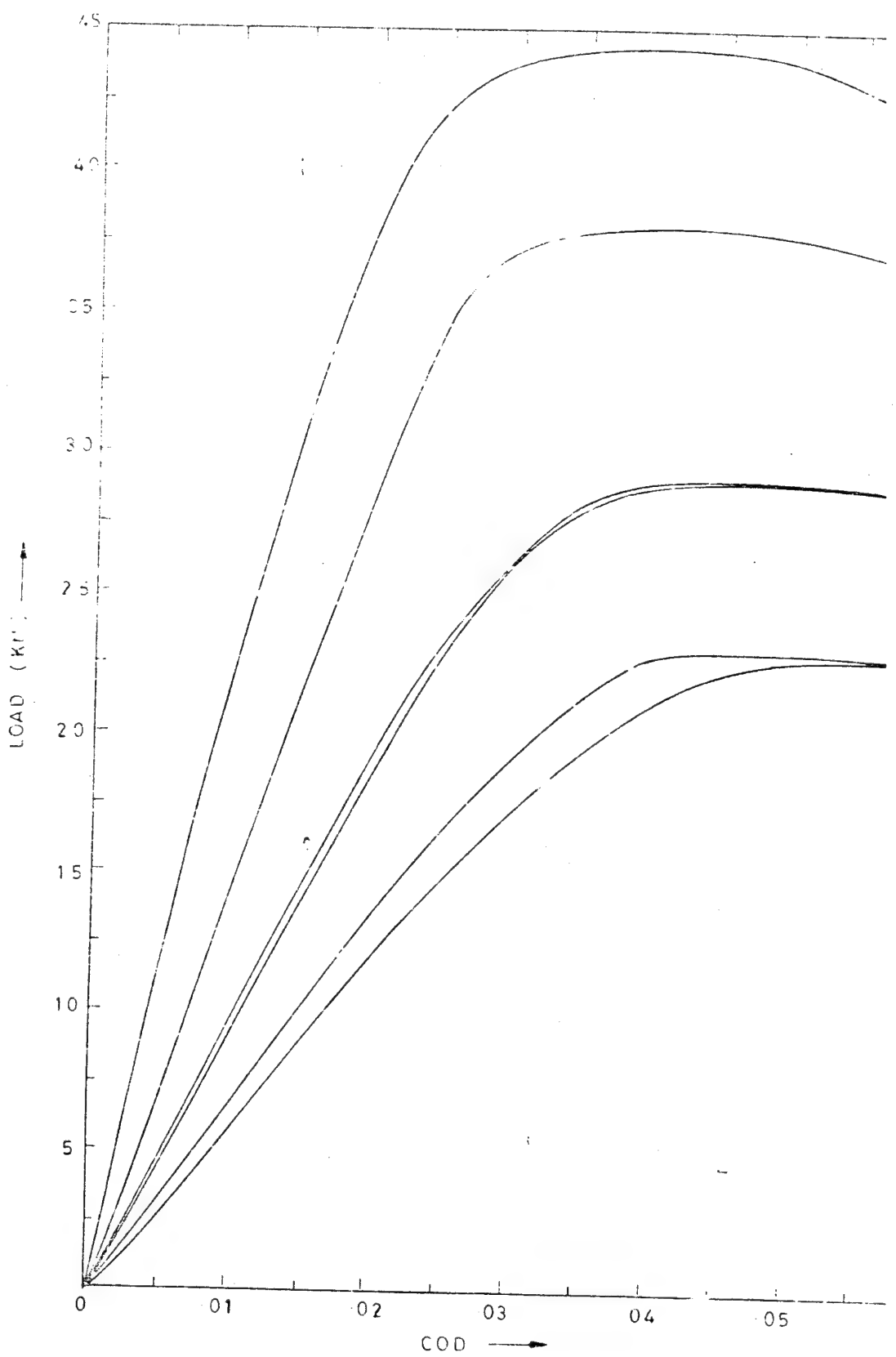


Fig. 3 . Load displacement record for laminate B.

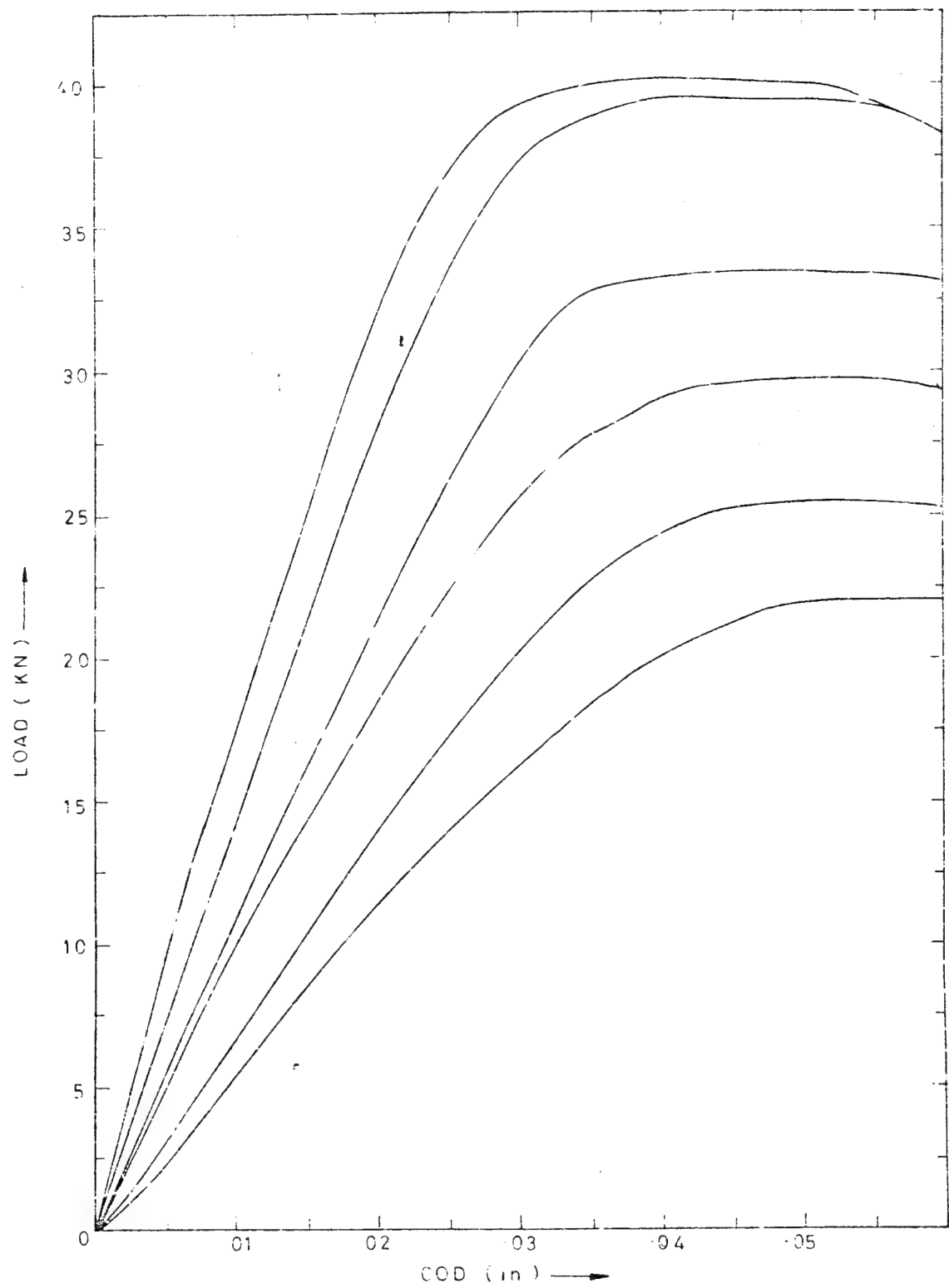


Fig. 4. Load displacement record for laminate C.

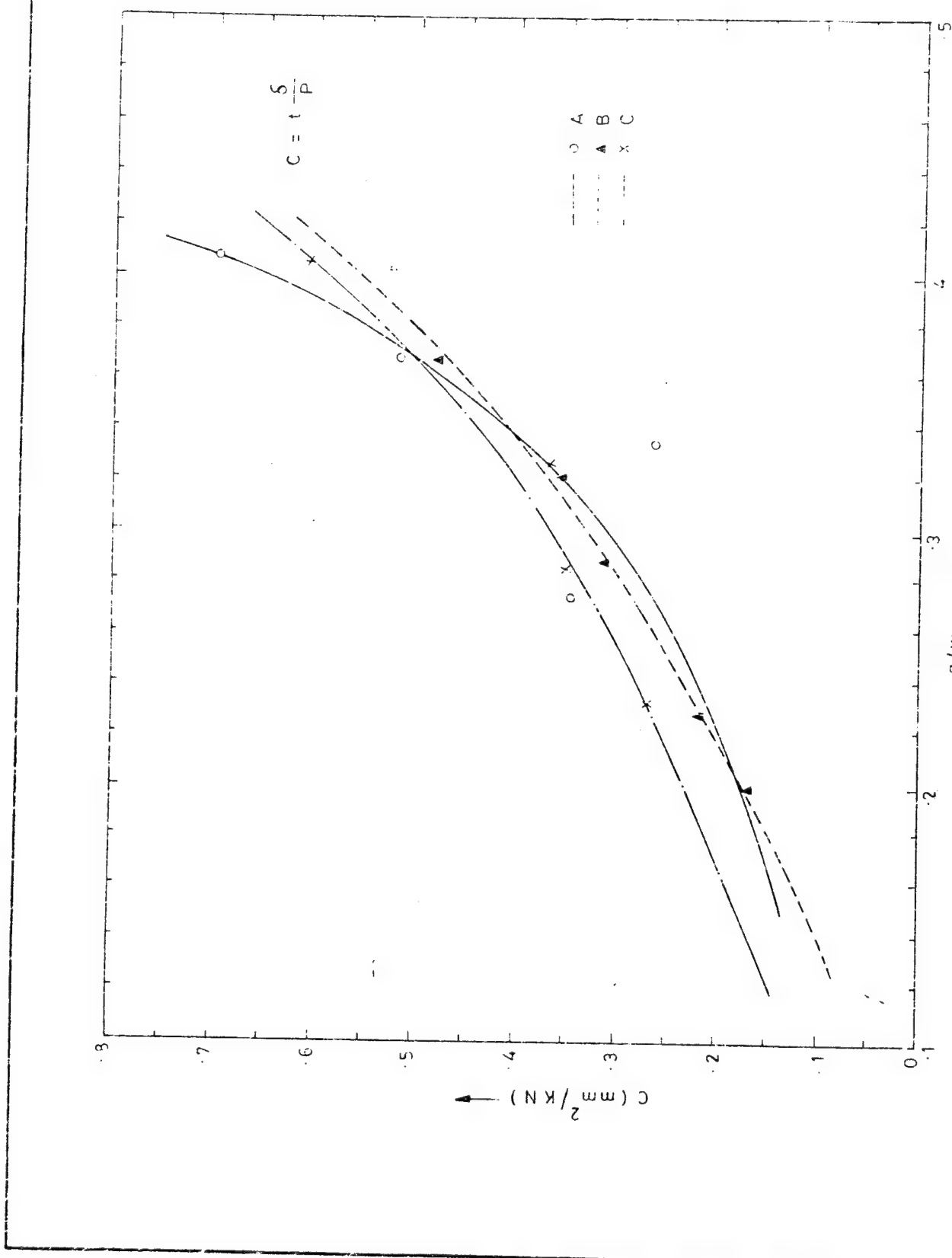


Fig. 5 . Crack detection compliance curve.

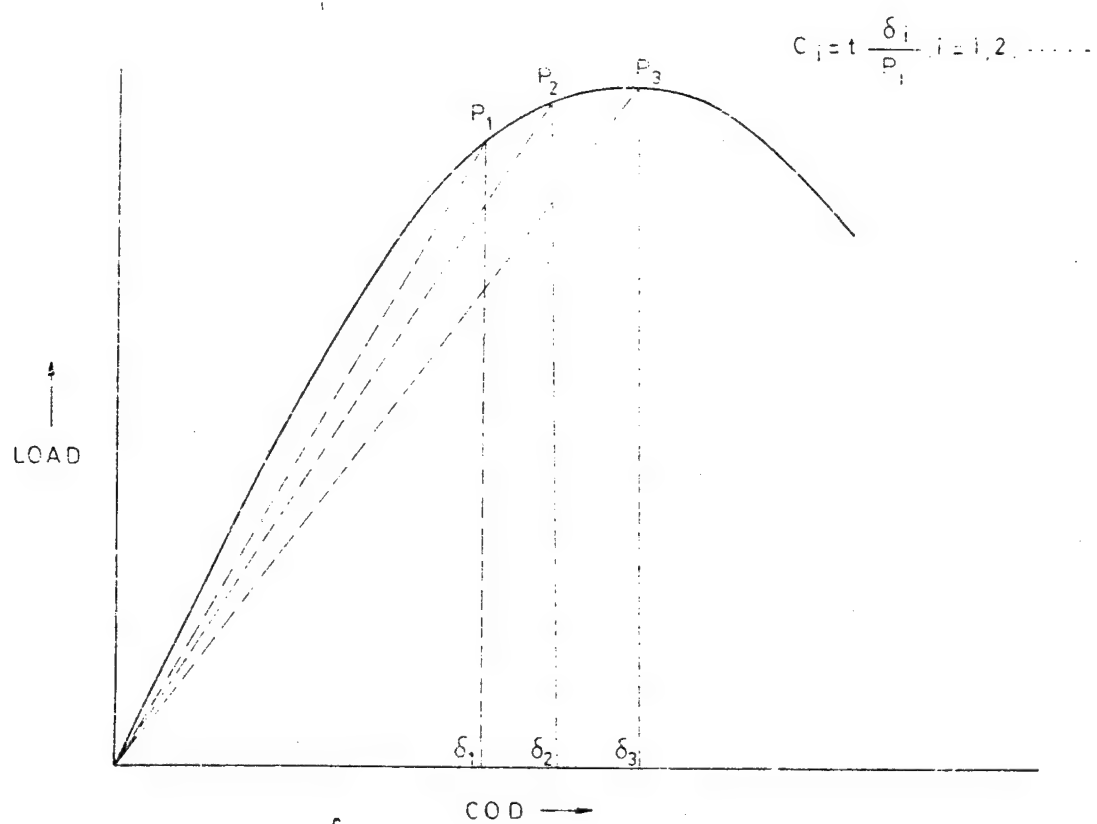


Fig. 6. Compliance determination.

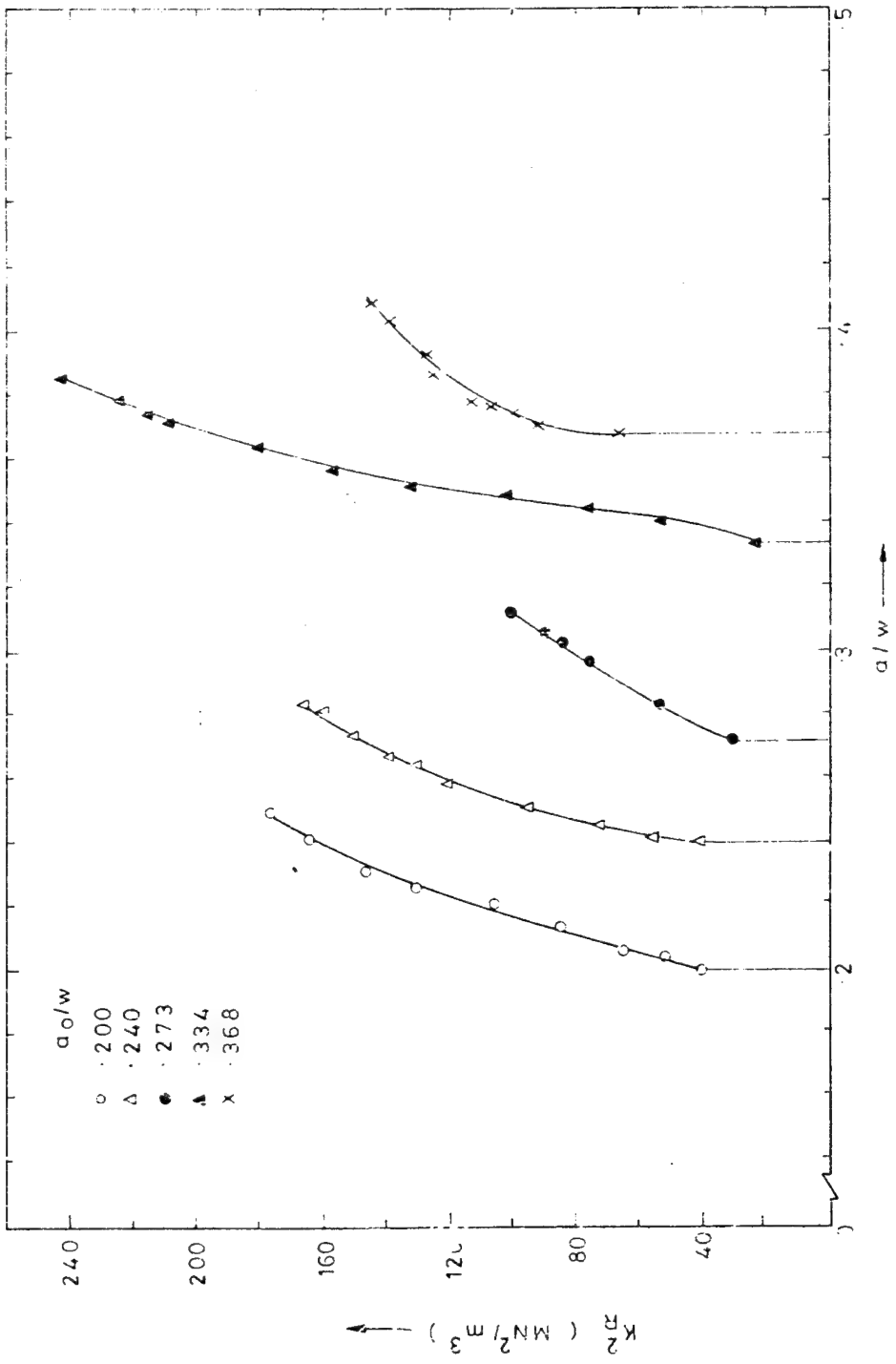


Fig. 7 . R - curve for laminates A .

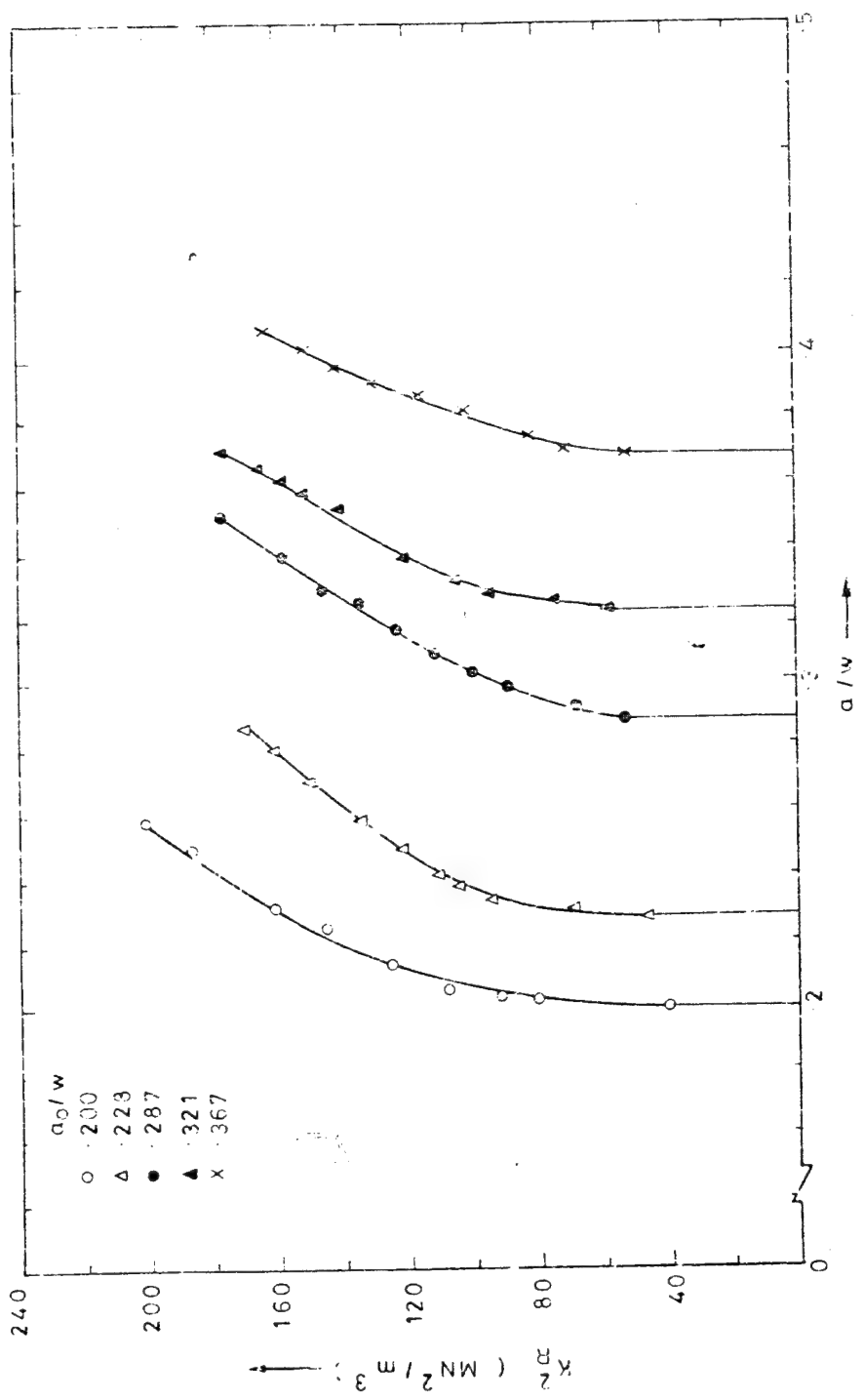


Fig. 8. R-curve for laminates B.

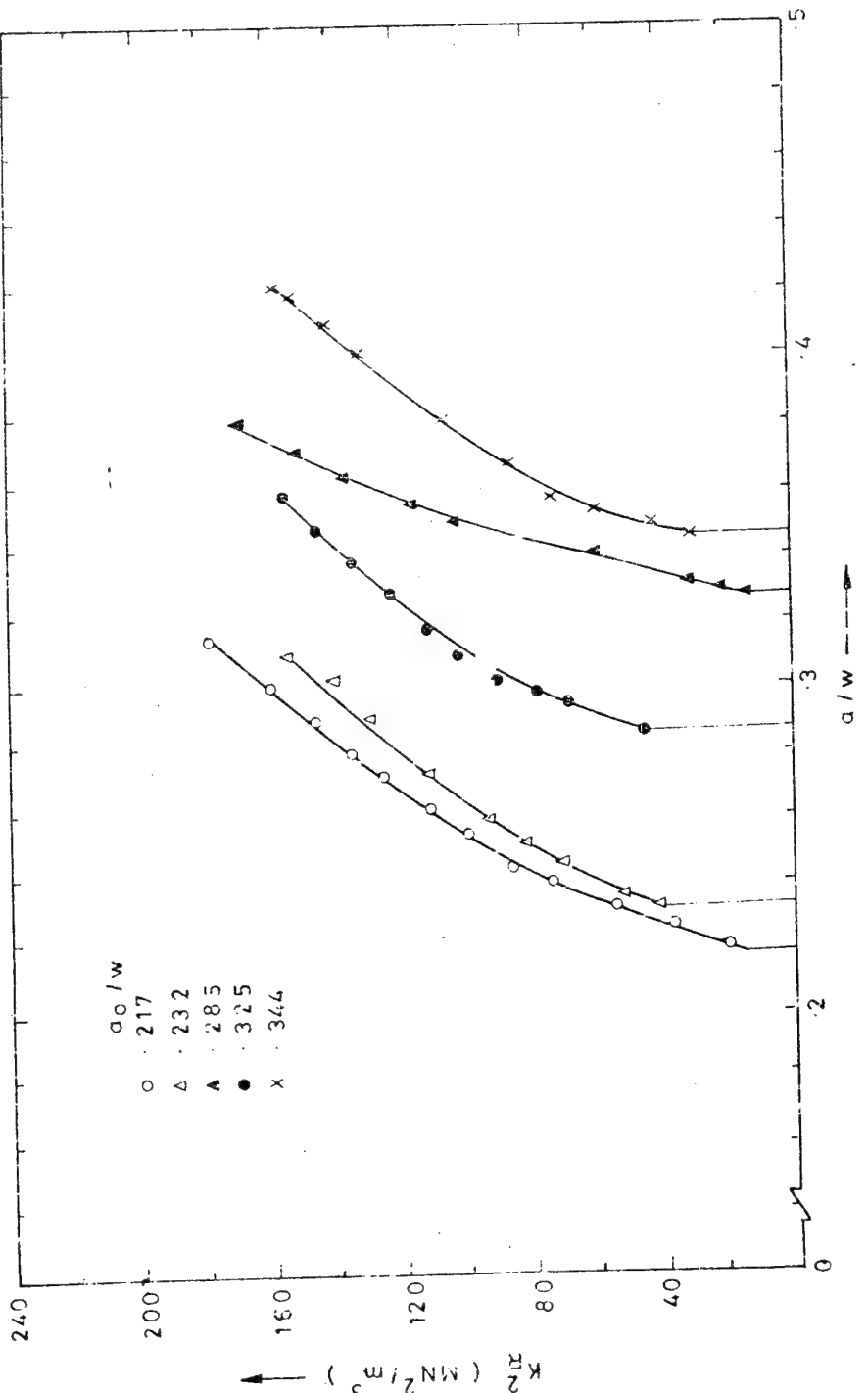


Fig. 9. R-curve for laminates C.

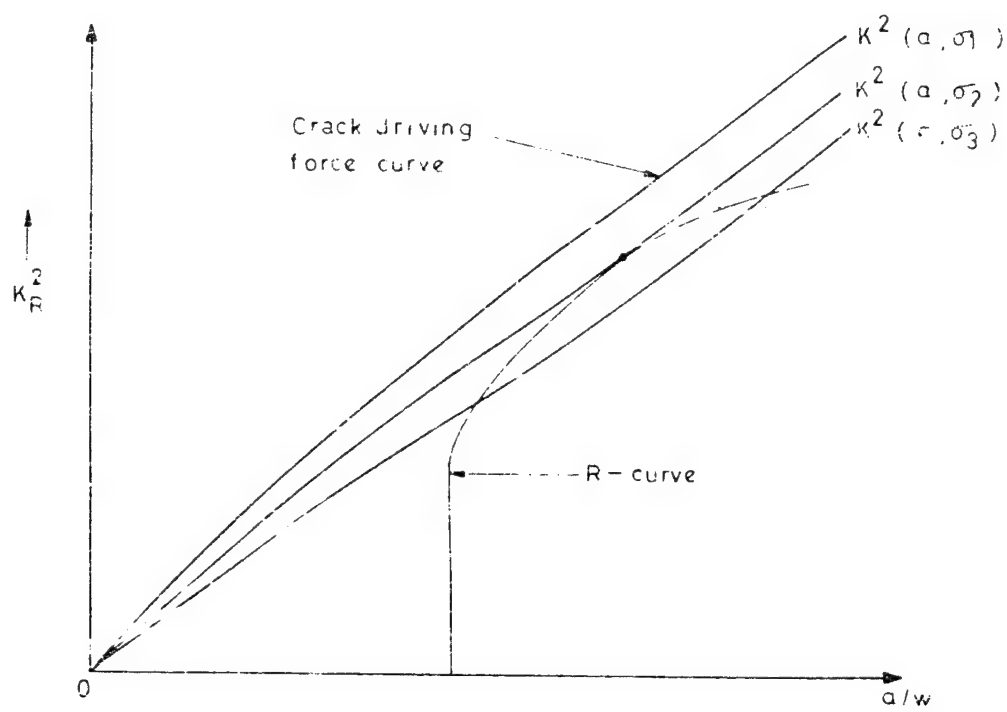


Fig. 10 . Schematic representation for determination
of crack instability from R - curve.

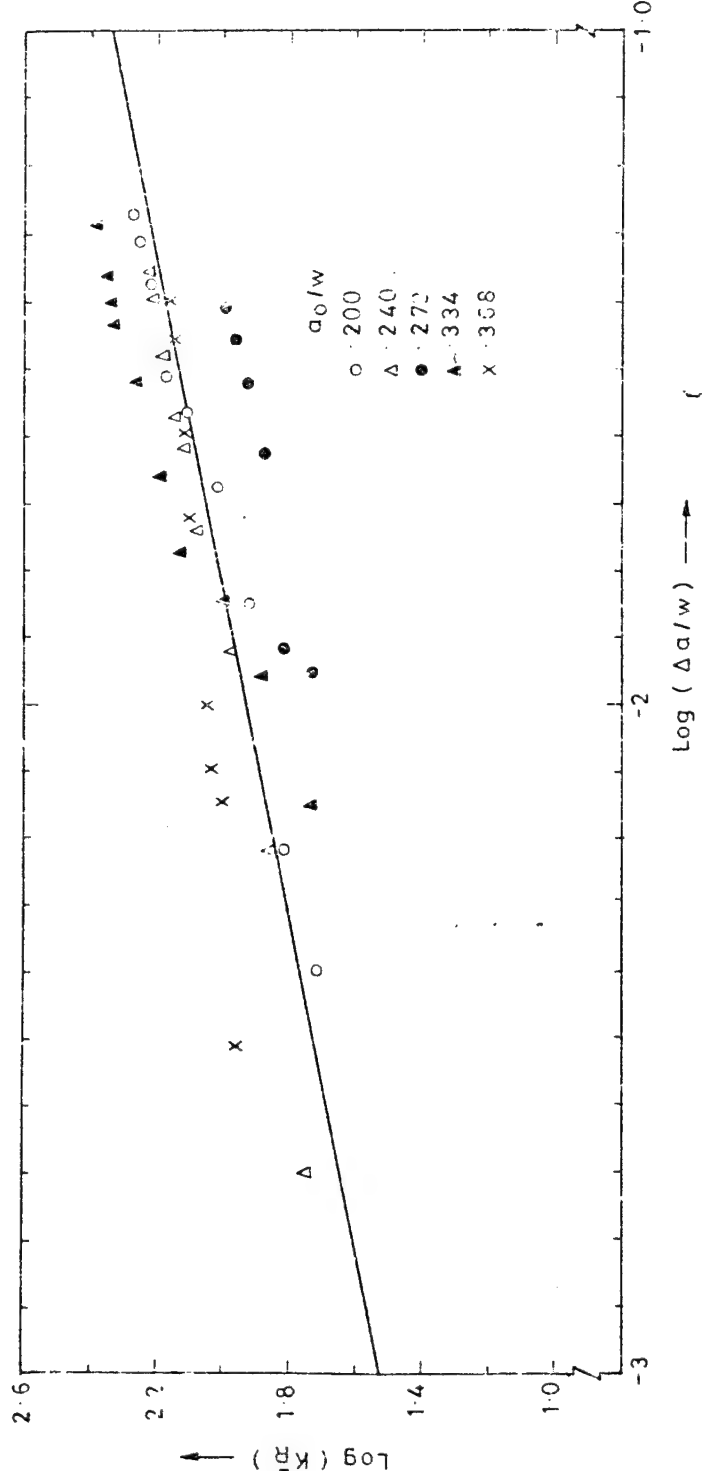


Fig. 11. K_R^2 as a function of crack extension for laminates A.

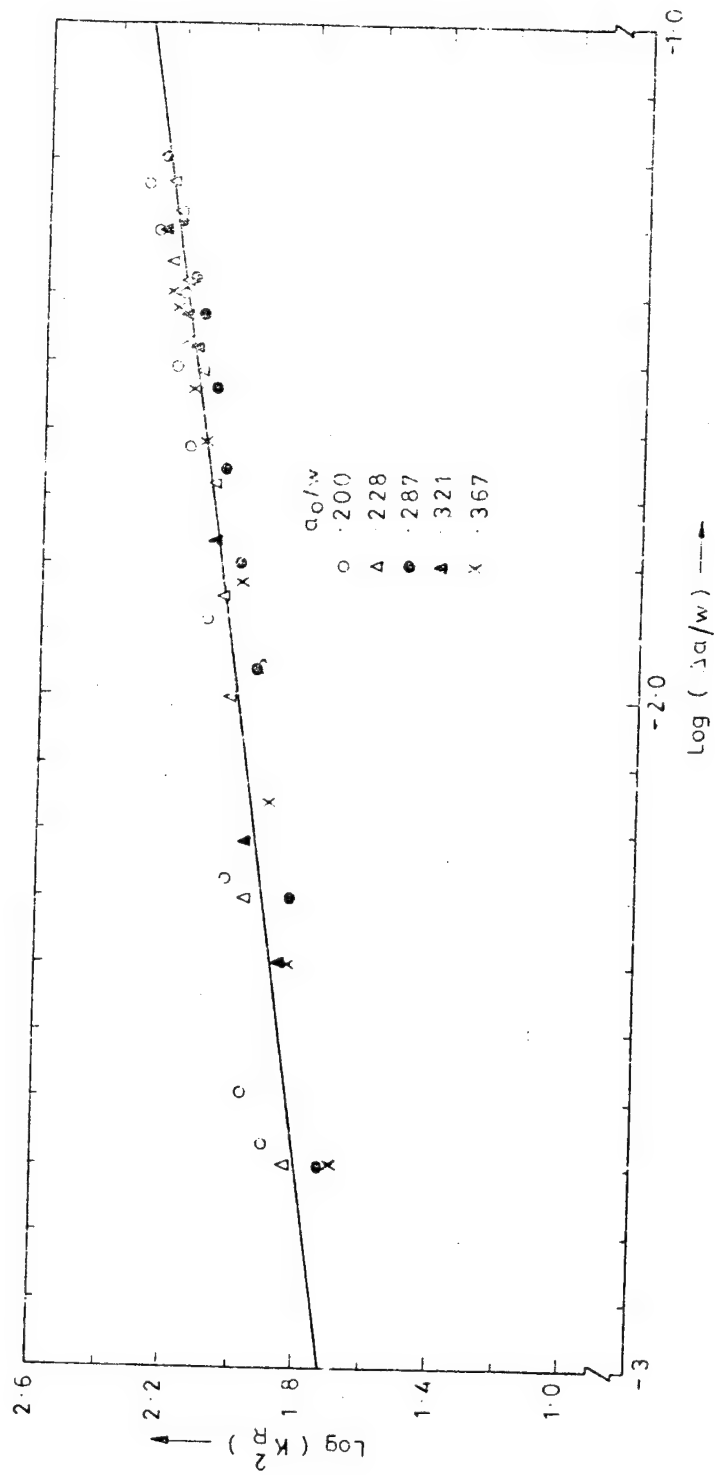


Fig. 12. K_R^2 as a function of crack extension for laminates B

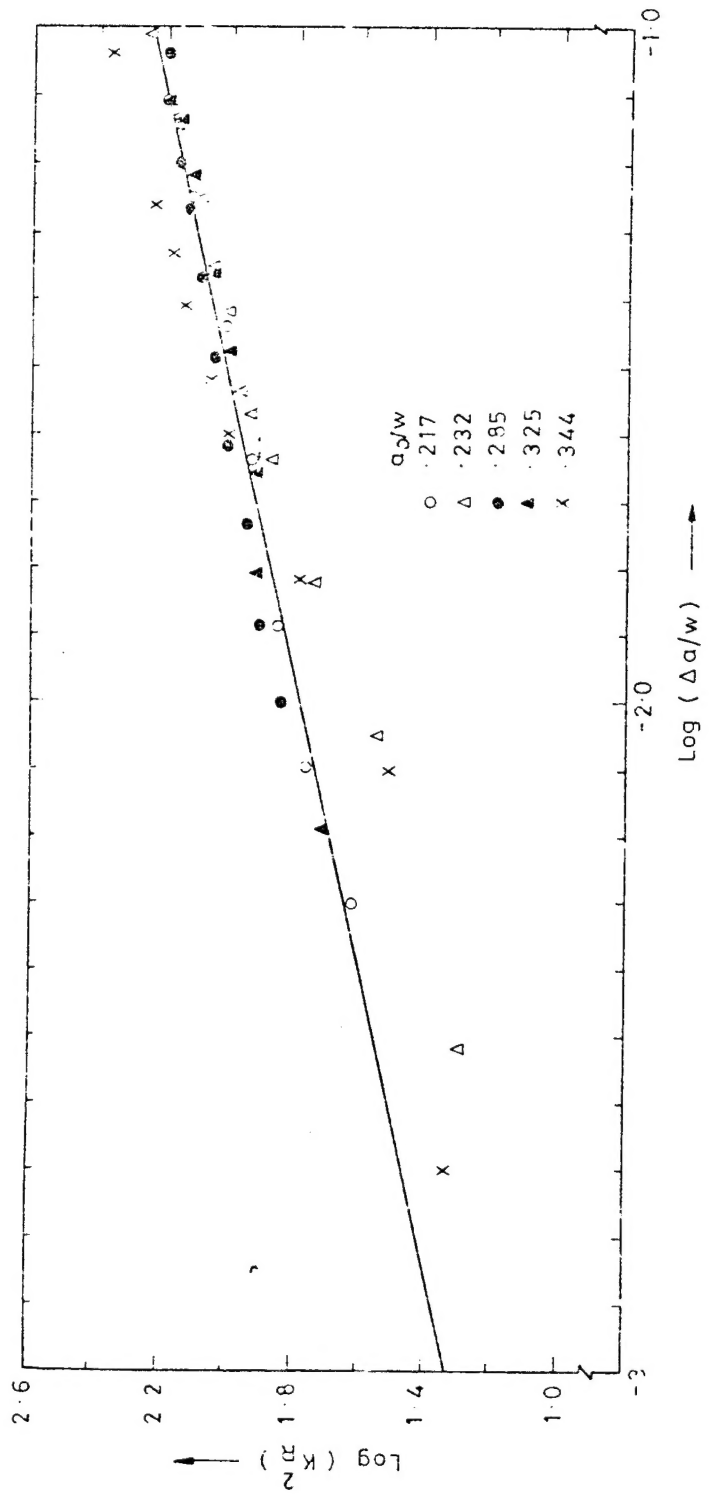


Fig. 13. K_R^2 as a function of crack extension for laminates C.

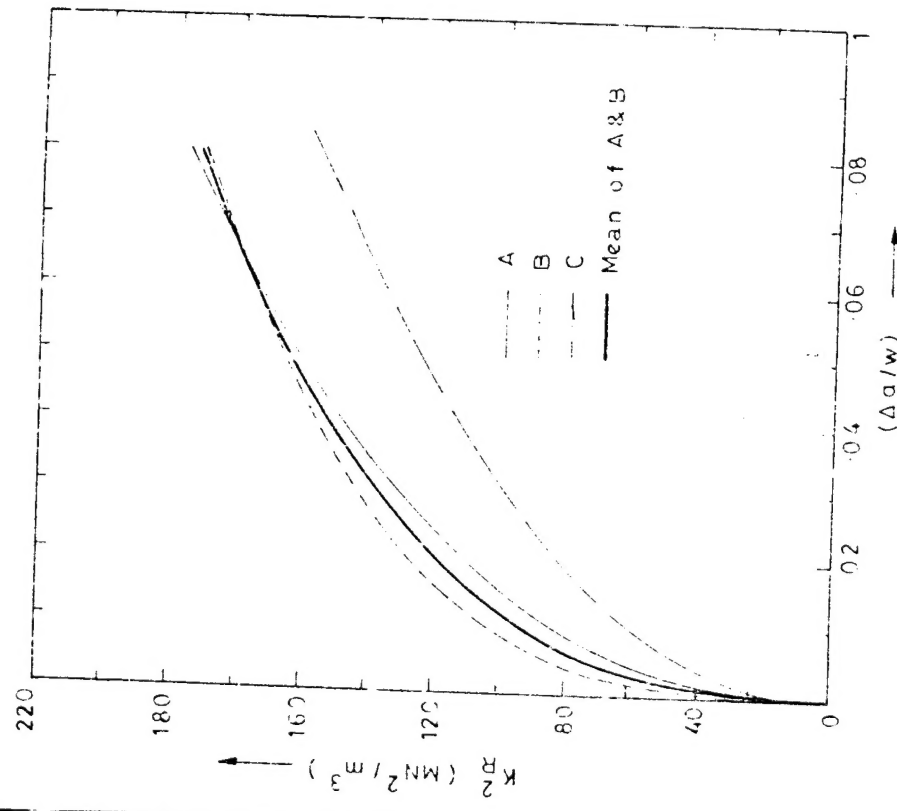


Fig. 14. R - curve S.

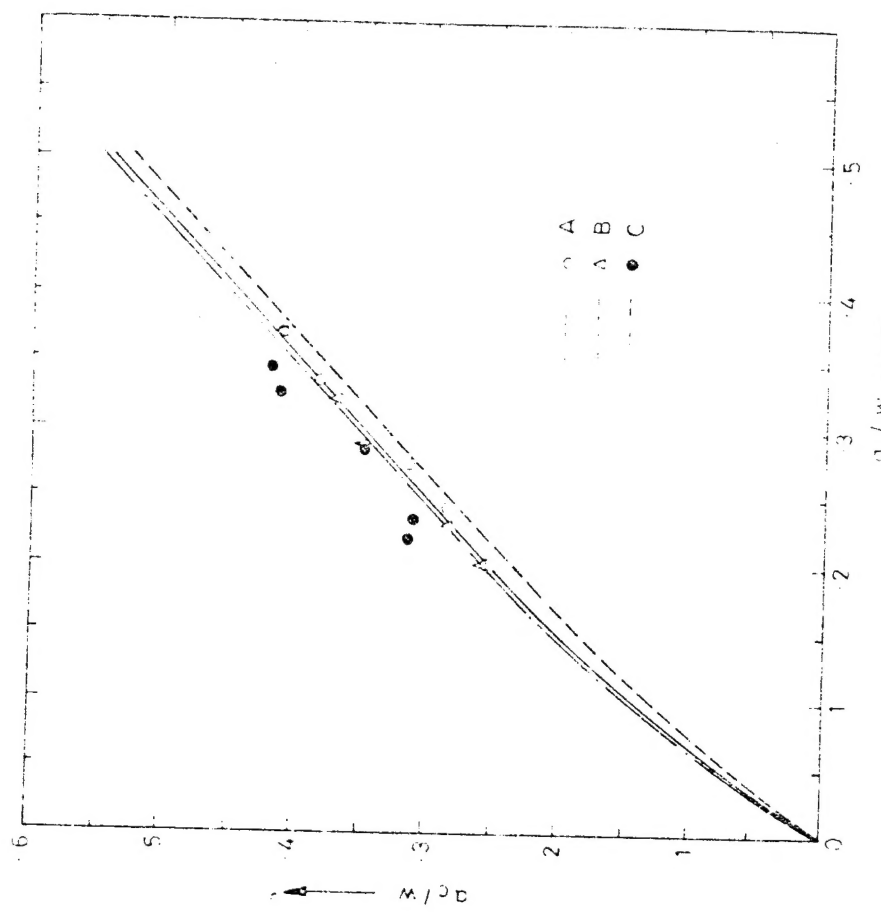


Fig. 15. Critical crack length a_c/w as a function of initial crack length a_0/w

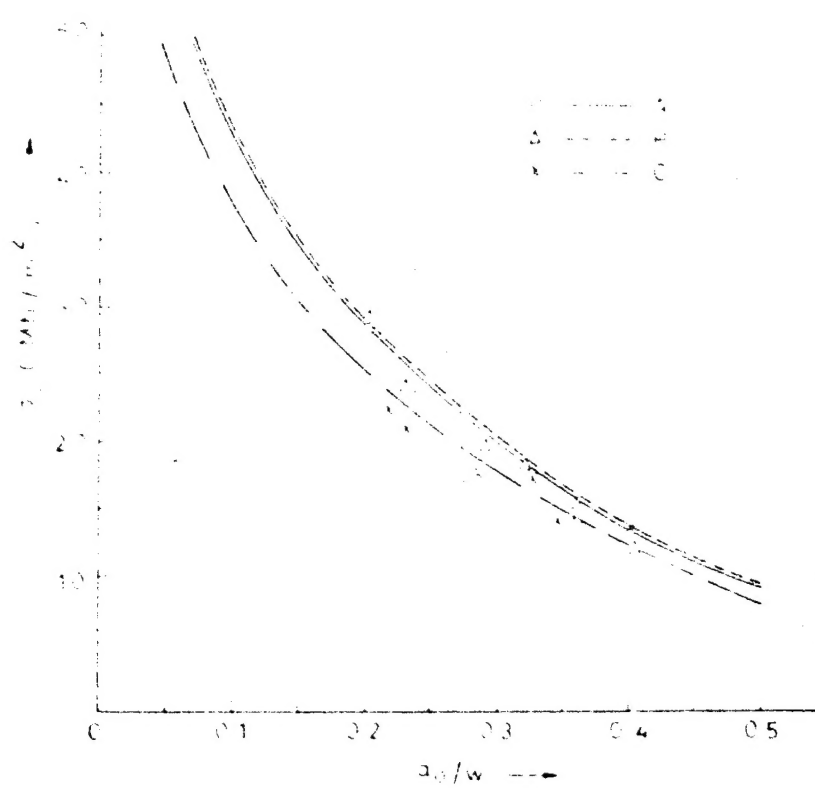


Fig. 16 Critical stress as function of a_0/w

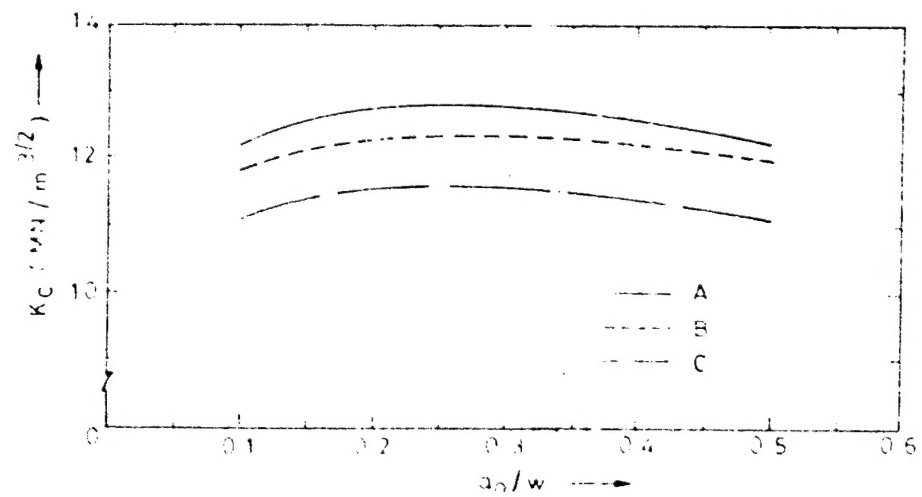


Fig. 17 Critical stress intensity factor as function of a_0/w

TABLE 3
Stress intensity factors

Panel	a	t	A_0	A_0/t	P_{max}	Rank	σ_c	K_{Ic}	K_{IS}	K_I	K_{II}
	mm	mm	mm ²	mm ³	kN		MN/m ^{3/2}				
A ₁	12.0	5.0	20.0	4.00	13.9	11.05	28.5	15.67	13.19	7.51	-0.48
A ₂	11.5	5.0	20.0	4.00	11.7	12.87	24.0	12.80	13.15	7.24	-0.22
A ₃	12.0	5.0	24.0	4.80	17.8	8.16	16.73	10.78	10.40	6.48	-0.39
A ₄	12.0	5.0	24.0	4.80	16.7	11.99	19.85	15.50	15.50	7.28	-0.51
A ₅	12.0	5.0	24.0	4.80	16.7	9.5	15.97	12.65	11.83	10.00	-0.36
A ₆	12.0	5.0	24.0	4.80	16.7	12.17	11.45				
						10.27		12.80	12.45		-0.43

B ₁	12.5	12.15	35.0	2.80	44.5	14.25	24.5	14.24	13.42	9.48	-0.44
B ₂	12.7	12.5	29.0	4.28	48.0	10.4	23.98	13.65	12.65	9.27	-0.52
B ₃	12.2	12.15	35.0	4.87	29.0	10.46	19.56	13.27	13.27	8.57	-0.63
B ₄	12.5	13.1	49.5	3.21	29.0	11.29	17.99	13.27	13.27	9.27	-0.49
B ₅	11.7	12.8	43.0	3.67	23.0	10.82	15.35	12.81	12.81	8.94	-0.41
B ₆	12.9	12.8	52.0	4.03	22.75	11.76	13.77				
						10.96		13.45	13.08		-0.50

C ₁	13.4	14.5	27.0	2.77	40.1	9.14	22.22	15.34	12.65	4.79	-0.63
C ₂	12.7	14.95	29.5	2.32	39.5	9.18	20.8	12.41	12.25	7.2	-0.14
C ₃	12.8	14.95	26.5	2.85	33.5	9.53	17.5	12.54	12.68	7.48	-0.63
C ₄	12.3	13.8	40.0	3.25	29.6	10.91	17.55	13.01	13.01	5.47	-0.55
C ₅	12.2	14.8	41.0	3.64	25.5	9.08	10.05	12.50	12.25	7.07	-0.62
C ₆	13.0	13.8	52.0	4.03	22.0	10.50	12.35				
						9.18		12.77	12.45		-0.65